

LBL-17943
EEB-W 84-10
W-166

To be submitted to the Journal of Solar Energy Engineering.

MEASUREMENT OF FENESTRATION NET ENERGY PERFORMANCE:
CONSIDERATIONS LEADING TO DEVELOPMENT OF THE MOBILE WINDOW
THERMAL TEST (MoWITT) FACILITY

J. H. Klems

Applied Science Division
Lawrence Berkeley Laboratory
University of California
Berkeley CA 94720, U.S.A.

May 1984

This work was supported by the Assistant Secretary for Conservation and Renewable Energy, Office of Building Energy Research and Development, Building Systems Division of the U.S. Department of Energy under Contract No. DE-AC03-76SF00098.

**Measurement of Fenestration Net Energy Performance:
Considerations Leading to Development of the Mobile Window
Thermal Test (MoWiTT) Facility**

J. H. Klems

Applied Science Division
Lawrence Berkeley Laboratory
University of California
Berkeley CA 94720

Abstract

The need for information about fenestration net energy performance under realistic conditions is discussed and methods of measuring it by means of a net energy balance are reviewed. A detailed consideration of the energy flows entering the energy balance on a building space and the effect of random measurement errors on the determination of fenestration performance is presented. Estimates of the error magnitudes are made for several hypothetical measurement situations and it is shown that a specialized, highly accurate test facility is necessary for reliable measurements on fenestration systems with thermal resistance in the range 2-10 times that of single glazing or shading coefficient less than 0.7. A test facility of this type, the MoWiTT, which has been built at Lawrence Berkeley Laboratory, is described. The effect of random errors in the MoWiTT is discussed and computer calculations of its performance are presented. The discussion shows that, for any measurement facility, random errors are most serious for nighttime

measurements, while systematic errors are most important for daytime measurements. It is concluded that, for the MoWITT, errors from both sources are expected to be small.

Introduction

There is a wide range of questions relating to the development and utilization of energy-efficient window systems which cannot be answered without a quantitative knowledge of fenestration thermal performance under realistic conditions. Examples of these are as follows:

- (1) What are the payback period and life cycle cost for adding an exterior venetian blind to a single-glazed window?
- (2) How should design specifications or building codes be written to optimize the energy-efficiency of fenestration systems without unnecessarily restricting architectural flexibility?
- (3) What are the most appropriate laboratory test methods to use in comparing the performance of alternative fenestration products?
- (4) Is it worthwhile to invest research effort in developing very highly insulating (for example, R-10) fenestration systems?

The current method of answering questions such as these utilizes calculations of average net energy costs/benefits which are based on the U-value and shading coefficient of the fenestration. These calculations, which are often embedded in building simulation models such as DOE-2¹ or BLAST², require numerous subsidiary assumptions and approximations to specify the actual conditions to which the fenestration is subjected and the way in

which these interact with the adjacent building space. The method by which fenestration U-values should be measured is somewhat controversial^{3,4,5}, and some systems, such as fenestrations with exterior venetian blinds, do not have a well-defined U-value. The validity of superposition of U-value and shading coefficient has been experimentally verified only for simple fenestration systems^{6,7}. In short, to go from measured U-values and shading coefficients to average net energy cost/benefit requires a theory with substantial physical content. To test this theory requires the ability to measure average net energy performance of fenestration systems under conditions representative of actual use.

There are several conceptual ways in which these measurements might be made:

- (1) Installation of test windows in actual buildings, measuring the energy inputs and using building simulation programs to extract the behavior of the fenestration.
- (2) Construction of a simplified test room in which the fenestration is mounted, with measurement of the energy inputs and calculation of the net heat balance from these inputs.
- (3) Design and construction of a specialized facility specifically tailored to the measurement of net energy performance.

Both method (1), which may be termed the "field test" approach, and method (2), which may be termed the "passive test cell", have been used many times. These measurements, examples of which are given in the references⁹⁻¹¹, have thus far failed to provide a definitive treatment of fenestration performance. Method (3) is a fresh look at the problem which goes

substantially beyond the state of the art of method (2) (and unfortunately requires greater complexity and expense). As will be seen, the key distinction is a direct measurement of envelope heat flow, which is not done in method (2).

A key consideration is the average net energy flow through the fenestration. For buildings operating in the heating mode, energy and economic optimization favor an average net energy gain, insofar as it is compatible with comfort and other constraints on the fenestration and building space; for buildings in the cooling mode, a net energy loss or minimized gain is desirable. Several strategies for accomplishing these goals are possible:

- (a) All peak energy flows may be minimized to produce a more uniform net energy flow, i.e., low shading coefficient and high R.
- (b) Thermal storage or other systems which distribute local heat flows in time and/or space may be employed to moderate the effects of peak loads or to allow favorable peak loads (e.g., winter solar gain) to offset unfavorable ones.
- (c) The fenestration system may be designed to maximize favorable peak loads while minimizing unfavorable ones. This explicitly "passive solar" strategy has the largest potential for energy savings, but may require fenestration management, special design features in the building, and/or seasonal changes to the system.

The ability to implement these strategies depends both on climate and the type of fenestration systems available. Strategy (a), which is frequently used in commercial buildings or in hot summer climates without large diurnal temperature swings, is limited by the fact that only rather low-R

fenestration systems are available. Both strategies (b) and (c) obviously seek to exploit diurnal swings in temperature and solar heat gain. Strategy (c) is also limited by the R-value of currently available fenestration systems. All of the strategies may use fenestration management to varying degrees, and all may be modified or improved by the use of daylight to reduce lighting energy consumption.

This points to the importance of fenestration performance measurements in situations where (1) R-values are high, (2) peak heat energy flows are small, (3) average net energy flows and fenestration impacts are much smaller than peak energy flows, or (4) average net energy flows result from combining large solar gains over relatively few hours with small-to-moderate thermal losses over many more hours. For fenestration performance measurement, all of these situations require either measuring a small signal or taking the difference of two large signals. This immediately raises the question of measurement accuracy and sources of error.

In this paper we consider the sources of error affecting fenestration performance measurements and show that only a specially-designed facility is likely to produce data of sufficient quality to settle all of the issues for which one would like to have answers. The facility required turns out to need much greater accuracy than one might expect.

A particular example of this type of facility has been built at Lawrence Berkeley Laboratory. It is called the Mobile Window Thermal Test (MoWiTT) Facility. The characteristics and expected performance of this facility are also presented.

Fenestration Energy Flows in Sunlit Spaces

Consider a fenestration system F forming part of the envelope of a closed building space, and let an imaginary surface E be located an infinitesimal distance beneath the interior surface of the envelope of the building space (a glossary of symbols used is given in Appendix A). By assumption, E completely encloses the building space with the exception of the area of F . (This discussion applies to vertical, horizontal, or tilted fenestration systems.) We assume that E has small holes through which air may pass (leaks) or through which climate control systems may move energy, and that these are sufficiently small or geometrically shielded so that we may neglect radiant or conducted energy transfer through them. Let W be the total energy flow rate through the fenestration, H be the total heat flow rate across the surface E , I be the rate of heat flow by (uncontrolled) air movement through the holes in E , and L_C be the rate at which heat is removed from the building space by the climate control system. (Internal loads such as lights are included in L_C .) All other energy flows are defined as positive flowing into the building space. Then if T is the mean temperature of all the mass contained inside E , C is the weighted average of the product of density and specific heat for that mass, and V is the volume of the building space, it follows from conservation of energy that

$$W(t) = CV \frac{dT}{dt} + L_C(t) - H(t) - I(t) . \quad (1)$$

It is instructive to consider some of the terms in this equation. The fenestration energy flow, W , consists of two parts, $W = Q_W + S_W$, where Q_W is the net heat flow from the innermost surface of the fenestration by

conduction, convection and radiation, and S_W is the net transmitted solar energy, i.e., the transmitted visible and short-wave infrared radiation (direct and diffuse) less the transmitted outgoing radiation (from back-reflection inside the building space). For fenestrations with an inner surface which is appreciably transparent to thermal infrared radiation, the net transmitted flow is taken to be contained in Q_W . We can further subdivide Q_W into Q_C , the part which is convectively (and conductively) transferred to or from the interior air, and Q_R , the part which is radiatively transferred to or from the interior surfaces of the building space.

The envelope heat flow, H , is a purely conductive flow since the surface E was taken to lie inside the solid comprising the envelope. If we consider the heat balance on the (infinitesimal) envelope layer inside E , we find that

$$H(t) = H_C(t) - Q_R(t) - S_W(t), \quad (2)$$

where H_C is the heat flow to the air by conduction and convection. Note that because this equation has been integrated over the surface E , terms involving interreflections or radiative exchanges between different parts of the envelope do not appear.

The heat-balance equation for the air and other mass inside the building space, while similar in form to Eq. (1), is quite different in content:

$$CV \frac{dT}{dt} = H_C(t) + Q_C(t) + I(t) - L_C(t). \quad (3)$$

It contains only Q_C , the conductive/convective part of the fenestration

energy flow; the radiative and solar gain parts, Q_R and S_W , enter only partially and indirectly through H_C as determined by Eq. (2).

This discussion allows us to state clearly the dilemma of fenestration performance measurement: Fenestration energy flows are not well-localized, but are distributed by a complex radiative and convective equilibrium process over the entire adjacent building space. To localize and simplify the energy flow processes (as is done in laboratory-scale measurement) one must replace this equilibrium with a different one, and one is unable to calculate reliably the effects of this replacement because of the complexity of the radiative-convective problem. In order to determine the energy costs or benefits for a fenestration system in a particular building, one needs to determine the effect on $L_C(t)$ averaged over time. However, if one directly measures this quantity the result is characteristic as much of the particular building space as of the fenestration, because of the indirect and partial manner in which the radiative and solar heat flows enter Eq.(3). In order to extract the fenestration performance under realistic conditions from a particular test situation one must determine all three components of the fenestration energy flow; yet each of the above equations contains at least one quantity which is very difficult to measure (H in Eqs. (1) and (2), H_C in Eq.(3)) in addition to the fenestration energy flows.

Error Analysis

Let us consider the effect of finite accuracy in measuring the terms on the right-hand side of Eq.(1). Assuming that the errors are random and uncorrelated, the fractional error in the fenestration energy flow is given

by

$$\frac{\delta W}{W} = \left\{ \left[\frac{\delta(CV \frac{dT}{dt})}{W} \right]^2 + \left[\frac{H}{W} \left(\frac{\delta H}{H} \right) \right]^2 + \left[\frac{I}{W} \left(\frac{\delta I}{I} \right) \right]^2 + \left[\frac{L_C}{W} \left(\frac{\delta L_C}{L_C} \right) \right]^2 \right\}^{1/2}, \quad (4)$$

where δW denotes the error in W , and similarly for the other quantities in the equation. The terms on the right-hand side of this equation arise respectively from the heat capacity of the air (etc.) inside the building space, envelope heat conduction, infiltration, and the climate-control system.

In order to estimate the magnitudes of the various terms in Eq.(4), we consider a simple model of the building space. We first parameterize the fenestration heat flows using (for nighttime heat loss) U_0 , the U -value for single glazing, a dimensionless thermal resistance, R , (defined as U_0/U for a fenestration of thermal transmittance U) the fenestration area, F , and the inside-outside air temperature difference, ΔT :

$$W = - \frac{F}{R} U_0 \Delta T. \quad (5a)$$

Similarly, for the daytime heat flow we use the shading coefficient, B , the heat flux through single glazing (solar heat gain factor), J_0 , and the fenestration area receiving direct sunlight, F' :

$$W = B J_0 F'. \quad (5b)$$

For simplicity, we neglect the comparatively small $U\Delta T$ term when the

fenestration is in the solar gain mode. Nighttime envelope heat flows are analogously defined, neglecting the effects of thermal lags:

$$H = -E \frac{U_0}{R_E} \Delta T, \quad (6a)$$

where E is the total envelope area excluding the fenestration and R_E is the dimensionless envelope resistance. We assume that in the daytime the envelope heat flow is dominated by the fenestration heat gain, a fraction, α , of which flows into the envelope rather than into the air of the building space:

$$H = -\alpha B J_0 F'. \quad (6b)$$

Infiltration is parameterized using the air exchange rate per unit time, a :

$$I = -C V a \Delta T. \quad (7)$$

Finally, the heat transferred by the climate control system is taken at nighttime to be

$$L_C = \zeta(W+H) + I + z_I G, \quad (8a)$$

where the parameter ζ is included to account for thermal lags, z_I is the internal load per unit floor area (from lights, etc.), and G is the gross floor area. The daytime space load is taken to be

$$L_C = (1-\alpha) B J_0 F' + \xi \Delta T_S \left(\frac{U_0}{R_E} \right) E + z_I G. \quad (8b)$$

Here ΔT_s is the temperature difference based on the sol-air temperature and ξ is the fraction of the envelope illuminated by sunlight.

Because the mean temperature of the air (and other thermal mass) inside the building space varies with time and is sampled only at finite intervals, there is an uncertainty associated with its heat content given by

$$\delta\left(cV\frac{dT}{dt}\right) = \frac{\sqrt{2}cV\delta T_A}{\tau}, \quad (9)$$

where τ is the sampling period and δT_A is the RMS error for an individual measurement of T .

With these equations it is possible to calculate the individual terms in Eq. (4), which are shown in Table 1. These are then added in quadrature to obtain $\delta W/W$. It can be seen that the errors contain ratios of building volume to fenestration area and envelope area to fenestration area. The relative magnitudes of errors from the different sources will therefore change with differing building size.

Error Estimates for Sample Buildings

Using the formulas in Table 1, we make numeric estimates for two prototypical buildings, a small one and a large one. For the small building we consider a 1500 square foot one-story residence with a glazing area equal to 20% of the floor area and half of it on the south side. For the large building we consider a seven-story office building with the dimensions of the Norris-Cotton Building,¹² but with a glazing area equal to 30% of the exterior wall area. These two examples are chosen to represent the range

of buildings in which one might do field tests of fenestration performance.

Each building is assumed to face due south, and daytime estimates are made for a clear winter day at noontime. Numerical values of $U_0 = 5.7\text{W/m}^2\text{K}$ and $J_0 = 800\text{W/m}^2$ are assumed. The latter corresponds to the solar heat gain for a south-facing window at noon on Jan. 21 at 40°N latitude. The inside-outside temperature difference is assumed to be 20°C , and the sol-air temperature is assumed to be 30°C above the outside air temperature. Both buildings are assumed to have a ventilation/infiltration rate of 0.75 air changes/hour. Other assumptions are $R_E = 20$, $V/F = 12.2\text{m}$, and $E/F = 18.5$ for the small building; $R_E = 17$, $V/F = 33\text{m}$, $E/F = 5$, $G/F = 58.3$ and $F'/F = 0.25$ for the large building. Internal heat sources are assumed to be zero for the small building and $z_I = 8.0\text{W/m}^2 (0.75\text{W/ft}^2)$ for the large one. Indoor air temperature measurements are assumed to be recorded hourly with an RMS error of $2^\circ\text{C}/\sqrt{2}$. It is also assumed that $\alpha = 0.4$.

The resulting error estimates are shown in Table 2. An example of how these estimates are used to derive measurement accuracy requirements in the following sections is given in Appendix B.

Limitations of Field Measurements

Examination of Table 2 yields some interesting insights into the usefulness of field measurements for determining fenestration performance. If we consider first the large building in the nighttime heating mode, Table 2 indicates that the HVAC system performance, air infiltration, internal temperature, and envelope heat flow may all be important sources of error. If we assume that we require an accuracy of at least 10% for the window heat flow, Table 2 implies (by the calculation outlined in Appendix B) that to

measure the nighttime heat loss through single glazing one would need to measure the HVAC system performance (L_c) to 3%, the infiltration rate to 3%, the envelope heat flow to 33% and the mean internal temperature to 0.4°C . For daytime measurements one would need to measure L_c to 2%, infiltration to 6%, envelope heat flow to 13% and mean internal temperature to 0.6°C . Attaining these accuracies in a large building with a complex HVAC system would be exceedingly difficult, to say the least.

Attaining the required accuracy on internal temperature would be particularly difficult, since it is the effective mean temperature of all the material inside E which must be determined. This requires accurate knowledge of both the temperature and thermal capacity of everything inside the surface that we have denoted E. For a large building considered as a single zone, this includes interior partitions, furnishings, etc. In Table 2, the space is assumed to contain only air; when these other masses are included, the internal heat content can easily become the dominant error source. If one restricts attention to a sub-zone to make this problem more tractable, then new uncertainties are introduced by heat and mass exchanges between zones, which were neglected in this analysis.

In short, measurement of heat transfer through unshaded single glazing turns out to be a difficult undertaking in a large building. It would clearly be a poor place to attempt measurements for systems with R or $1/B$ in the range 2 - 10.

In the case of the one-story residence, use of electric heating makes it possible to attain a very small value for $(\delta L_c/L_c)$, so that errors from this source may be neglected. (This may not be the case for cooling, however.) Table 2 then indicates that the dominant error source is envelope

heat conduction, followed closely by air infiltration. To measure the heat loss through single glazing requires that the envelope heat flow be known to 5% and the air infiltration be known to 9%. The latter requirement is certainly attainable, although it would require continuous monitoring of the air infiltration rate. Attaining the former is more difficult, since the accuracy requirement is on the heat flow integrated over the entire exterior envelope (excluding the fenestration) rather than on the localized heat flux. This is a formidable measurement problem, since it must take account of inhomogeneities in construction and variations in material properties. Uncertainties from these sources are notoriously difficult to eliminate in an existing building.

We conclude that isolation of the thermal energy flows through fenestration in an existing building, built with standard construction techniques, is difficult even for unshaded single glazing and rapidly becomes unfeasible as R increases or B decreases. The analysis presented here indicates that one would be doing well to measure even unshaded single glazing performance to an accuracy of 10% in a large building. For a small residence the practical limit is probably somewhere between 1 and 2 for R and between 1 and 0.7 for shading coefficient.

Two additional considerations not included in this analysis further argue against field testing as a method of determining fenestration performance. First, in reality one must know dynamic envelope properties rather than the static ones used in the simplified analysis. Second, measurements in a building will mix the contributions of fenestrations in different orientations performing in different modes, for example, south-facing in a direct gain mode and north-facing in a diffuse gain/thermal loss mode. Attempting

to separate these by zoning re-introduces the problems of interzone energy transfers.

Error Estimates for a Passive Test Cell

We next consider the accuracy attainable using a passive test cell. We consider a cell 2.4 m high by 2.4 m by 3 m (8 ft x 10 ft x 8 ft high), with a fenestration system mounted in a short side and facing south. A residential-sized fenestration of 1 m² area and a large fenestration filling the entire 2.4 m square are considered. The R value of the envelope is taken to be 40 and it is assumed that the cell is so tightly constructed that the infiltration rate is negligible. The magnitudes of the potential error sources are then shown in Table 3. We note that for the small window the fenestration area is 17% of the floor area, which, while high, is in a reasonable range for residential buildings. The large window is 80% of the floor area, which is atypically large for most kinds of construction.

The roughly equal importance of accuracy in measuring the climate-control system performance and the envelope heat conduction immediately emerges from the table. In the nighttime heating mode, in order to measure a residential-sized single-glazed window to 10% accuracy requires a 6% measurement of H; for an R-10 system one would need 0.6%, which is probably not possible. For the large window the situation is somewhat better; a 10% measurement of H would permit nighttime measurements on a system with R = 4. A measurement of H is equally important for daytime measurements on both size fenestrations.

This has awkward implications for window performance measurement. Using a simple passive cell, it would appear that for residential-sized windows one

can accurately study only low-thermal-resistance fenestration systems. If one wishes to study the high-R systems which are of interest for improving building energy- efficiency, one must study large windows. This compromises the aim of studying realistic fenestration performance somewhat, since the glazing-to-floor area ratio will be atypically high (and therefore the importance of radiative heat transfers will be exaggerated).

These conclusions arise from the nighttime heat flows. A model which neglects thermal storage effects cannot adequately deal with daytime heat flows; in the above it has been assumed that $\alpha = 0.4$, which is a value made plausible by more detailed calculations presented below. In addition, the simplified model is purely one-dimensional, whereas the daytime heat flows arise from highly inhomogeneous distributions of solar flux on the interior surfaces. This effect is also present to a lesser degree in the nighttime heat flows, due to the radiative coupling to the fenestration.

These limitations of the model mean that Table 3 should be interpreted as presenting approximate lower bounds on the errors: effects left out of the model may add additional error, but will not greatly reduce those sources identified in the table. For example, it would be correct to conclude from Table 3 that envelope heat flows represent a significant potential source of error in both daytime and nighttime measurements, and that one should be increasingly critical of fenestration measurement procedures as R or $(1/B)$ increase. However, it would be dangerous to conclude that, since Table 3 indicates that only modest accuracies for H (~15%) are necessary to measure daytime flows through large fenestration areas, a technique of modest accuracy, such as calculation of H using a simulation program, would be adequate.

A Specialized Facility for Measuring Fenestration Energy Flow

The foregoing considerations make clear the capabilities which a facility designed to measure fenestration performance should have. First, it should measure fenestration performance under conditions as representative of actual use as possible. This means that the fenestration should be exposed to outdoor weather conditions, since the combined effects of wind and radiation from the sun, sky and ground cannot be adequately simulated in the laboratory. It should be possible to measure fenestrations in different orientations and climates. The interior space should be room-like, with the correct height (since convective processes do not scale) and have a ratio of fenestration dimensions to room dimensions reasonably like those in a building (so that radiative processes have the correct weight). Surface reflectivities and emissivities on the interior should also be similar to those in a building, and it would be preferable to have them be variable. The fraction of solar-optical radiation absorbed in the interior envelope surfaces which is promptly transferred into the air should be comparable to that in a building. This means that the envelope should have a building-like thermal time constant. Ideally the thermal time constant should be variable. The air temperature in the space should be kept within a reasonable comfort range, and humidity and forced-air velocities should be in a range representative of a building.

Second, the net energy flow, W , through the fenestration should be measurable with a time constant similar to the intrinsic response of the fenestration, i.e., very short. This means that the air infiltration rate must be very small or accurately measured, and heat added to or removed from the air by the climate-control system should be accurately monitored. Internal

loads, if present, should be accurately measured. The area-integrated conductive heat flow through the interior surface should be accurately determined. The mean temperature of the air and any interior thermal mass should also be measured.

Third, it should be possible to do a wide variety of experiments in the facility, in order to relate the fenestration net energy flows to explanatory variables such as temperatures, solar intensities and wind speeds

The Mobile Window Thermal Test (MoWiTT) Facility

A measurement facility approximating these requirements has been built at Lawrence Berkeley Laboratory. It is called the MoWiTT (Mobile Window Thermal Test) facility and is shown in Fig. 1. It consists of one or more mobile measurement modules, together with a central instrumentation van for data collection. Each module contains a pair of identical test rooms, each with a removable exterior wall and roof panel. This allows direct comparative measurements between either horizontal or vertical fenestration systems exposed to the same exterior weather conditions. A variable climate is achieved by moving the MoWiTT to the climate of interest.

Realistic interior conditions are achieved by making the test room dimensions and construction as nearly like those of a room as possible. The interior dimensions of 2.44 m parallel to the removable wall by 3.05 m perpendicular to it by 2.34 m high provide a space of the correct height and reasonable proportions, although the room is smaller than typical for a normal residence. The walls are of plywood-faced polyurethane panels, providing a thermal time constant similar to light-frame residential construction. The room is designed to permit the addition of thermal mass for

simulation of higher-mass structures. Wall, ceiling, and floor surface treatments may be varied to achieve the correct emissivity and reflectivity, or, alternatively, to study the effect of these parameters on the fenestration performance. The climate-control system for each test room is self-contained and may supply either heating or cooling.

After realism, the key consideration in the MoWiTT design was measurement accuracy. Since both high-resistance and low-shading-coefficient fenestration systems are of interest, the ability to measure the performance of a 1-m^2 fenestration system with $R = 10$ (i.e., ten times the resistance of single glazing) or $B=0.1$ to an accuracy of 10% was a design goal.

Experimental flexibility is achieved by having a large data-recording capacity together with a flexible computer system for collecting and manipulating the data. Provision has been made for bringing signals from up to 150 sensors out of each test room, with an additional 50 sensors per room mountable on the exterior side of the fenestration. These are connected through a multiplexer to an LSI-11 computer. Data from temperature sensors, anemometers, radiometers, or other instrumentation may be collected. The data are recorded on disc. When in the field, data may be sent back to the laboratory either on floppy disc or by telephone. The computer may also be used to control devices inside the test rooms (for example, the operation of blinds during an experiment on window management) or to modify the chamber or guard conditions.

Measurement Accuracy in the MoWiTT

Let us consider how the MoWiTT design accuracy is achieved. Examination of the error sources for the passive cell in Table 3 (which is the same size

as a MoWiTT test room) points up the magnitude of the problem. Even with the high level of envelope insulation, a 1% measurement accuracy on the area-integrated envelope heat flow would be necessary for nighttime measurements. Considering that heat fluxes will be spatially inhomogeneous, due to the effects of radiation and convection, it seemed highly unlikely that measurements could be made to this accuracy.

This problem is solved in the MoWiTT by surrounding the two test rooms with a guard plenum through which controlled-temperature air is circulated as shown in Fig. 2. This has the effect of decoupling the envelope heat flow from the external temperature and greatly reducing its magnitude during nighttime measurements. It also makes all envelope surfaces (other than that containing the test sample) effectively interior surfaces, which is a better simulation of commercial and residential spaces (other than corner rooms) than is a passive cell. The contribution to the fractional error in the fenestration heat flow due to H then becomes:

$$\left[\frac{\delta W}{W} \right]_H = \frac{R}{R_E} \left(\frac{E}{F} \right) \frac{\Delta T_G}{\Delta T} \left(\frac{\delta H}{H} \right), \quad (10)$$

where ΔT_G is the temperature difference between the guard air and the air in the test room. The quantity ΔT is, as before, the inside-outside air temperature difference. As can be seen, the sensitivity of the fractional error $(\delta W/W)$ to the heat flow measurement accuracy $(\delta H/H)$ is reduced by a factor $(\Delta T_G/\Delta T)$. By maintaining the guard temperature close to the test room air temperature, we can make this factor small. We have taken it to have a value of 0.1 in making error estimates.

The presence of the guard reduces the effect of errors from a number of sources by the same factor. Table 4 summarizes the contributions to $\delta W/W$ from each of the four sources of error. From this table it can be seen that, with the guard, achieving the nighttime design goal requires a 5% accuracy for the climate-control system and the envelope heat flow measurement, knowledge of the air infiltration rate to an accuracy of ± 0.05 air changes per hour, and knowledge of the interior mean temperature to $\pm 0.05^\circ\text{C}$. These are achievable requirements.

Measurement of the area-integrated envelope heat flow, H , is achieved by lining the interior surfaces of each test room with large-area heat-flow sensors, as shown in Fig. 1(c). These sensors were specifically developed for this application^{13,14} and provide about 90% coverage of the interior surfaces. Tests on prototypes reported in Ref. 14 indicated that the sensors would have adequate accuracy, and preliminary tests on the full-size production models are promising.¹⁵

All electrical inputs to each test room are monitored using specially-constructed, accurate AC wattmeters that are insensitive to phase angle or waveform. This allows a measurement of the power delivered both to the electric heater and the circulating fan which has an accuracy better than 1%. Since the test room will not generally operate in the cooling mode for winter nighttime measurements, the 5% requirement will usually not apply; Table 4 indicates that daytime measurements require an accuracy in the 10 - 20% range. While this is not a difficult requirement when loads are large, it becomes more so when loads are small. In order to achieve good accuracy in measuring the heat extracted by the cooling system, the MoWiTT extracts heat from each test room with a liquid-to-air heat

exchanger. The flow rate, f , of the cooling fluid together with the fluid temperature where it enters (T_i) and leaves (T_e) the test room are measured, and the extracted heat is computed from:

$$L_C = \rho C_p f (T_e - T_i),$$

where ρ and C_p are the density and specific heat of the fluid, respectively. The percentage error arising from this measurement system is:

$$\frac{\delta L_C}{L_C} = \left[\left[\frac{\delta(\rho C_p)}{\rho C_p} \right]^2 + \left[\frac{\delta f}{f} \right]^2 + 2 \left[\frac{\delta T}{T_e - T_i} \right]^2 \right]^{1/2}.$$

One can see from this that accuracy from this system gets progressively worse as loads become small, since either f or $(T_e - T_i)$ becomes small while the measurement error does not. With the present MoWiTT measurement system, design accuracy can be maintained down to a cooling load of around 50W; for smaller loads, improvement in accuracy will be needed.

Through careful sealing of the test rooms, inadvertant air infiltration rates are reduced considerably below 0.05 air exchanges per hour, eliminating this source of uncertainty. Since there is a considerable pressure difference between the guard and each test room, sealing is quite important, and gasketing of the access doors and sample holding frame has been carefully engineered. For the same reason, the infiltration rate through the room envelope is independent of the outdoor pressure.

Through use of calibrated thermistors, individual temperature

measurement accuracies better than 0.05°C are attainable. Measurement of an accurate mean interior temperature, T_A , then becomes a question of correct placement of thermistors and sampling of temperatures. Since the MoWiTT has the capacity to record many thermistors and to sample them frequently, this requirement presents no insuperable problems.

Computer Calculation of MoWiTT Performance

In the foregoing discussion we have concentrated on nighttime measurements, with daytime estimates relying on the ad hoc parameter, α , the fraction of solar gain conducted through the envelope of the test room, which was taken without justification to have a value of 0.4. This procedure was used because a simple model such as the one used above is completely inadequate for calculating daytime performance of the test space.

We next turn to a computer simulation of the MoWiTT performance. This is done for two reasons: First, we wish to check the conclusions about accuracy reached on the basis of the simple model. Second, we would like to know how well the MoWiTT, with its active guard and large-area heat-flow sensors, performs in comparison to a more modest and conservative system.

We have therefore simulated the performance of two measurement facilities: (a) one test room of the MoWiTT, and (b) a passive test cell of identical size and construction, but without the active air guard space and large-area heat-flow sensors. As Eq. (1) shows, it is not possible to construct the window net energy flow without a knowledge of $H(t)$, the envelope heat flow. Accordingly, we add a network of commercial heat flux sensors to the hypothetical passive cell. These are arranged on a rectangular grid on each interior surface, with a vertical spacing of 1.2-m (4 ft) and a

horizontal spacing of 0.6 m (2 ft). On the floor and ceiling the 0.6 m spacing is along the direction perpendicular to the fenestration. (This network requires some 55 commercial heat flow sensors).

The program BLAST was used to perform the simulation because it does an hourly net heat balance and calculates the heat fluxes into each interior surface. Both the MoWiTT and the passive cell were assumed to have a triple-glazed window mounted in the sample wall. A cold, clear design day (Dec. 20) at Donner Summit, in the Sierra-Nevada mountains of California, was assumed. The transmitted solar energy and outdoor temperature assumed in the calculation are shown in Fig. 3(a).

The purpose of this calculation was to simulate the measurement process in each facility, assuming that the loads and envelope heat fluxes calculated by BLAST are the true ones. Infiltration and changes in air heat content were neglected in the calculation, reducing the measured variables to the space load, L_C , and the envelope heat flow, H . It was assumed that L_C could be measured to 5% accuracy in both facilities, and both the large-area heat-flow sensors and the commercial heat-flow sensors were also assumed to have 5% accuracy.

For the passive cell, one additional step was needed in the calculation. BLAST treats each envelope surface as a one-dimensional problem, by averaging solar and radiative fluxes over the entire surface. While this is a reasonable approximation for the MoWiTT, where the area-integrated heat flow is measured directly, it does not treat correctly the discrete heat-flow sensor network of the passive cell. Accordingly, for each hour of daylight the location of the moving patch of directly transmitted solar gain was computed by hand and it was determined which heat-flow sensors

were directly illuminated. Approximate values of the heat flux passing through those heat-flow sensors were computed from the transmitted solar intensity and the surface heat flux computed by BLAST. The values of the heat flux seen by the other sensors on the illuminated wall were corrected for the fact that part of the solar radiation was concentrated in the directly illuminated spot. The area-weighted sum of the heat fluxes was taken to be the contribution to $H(t)$ from that surface. Corrections to the radiative heat balance, due to the fact that surface temperatures in the directly illuminated spot will be higher than the mean temperature used by BLAST, were neglected for both the MoWiTT and the passive cell.

The results of the calculation are shown in Figs. 3 (b), (c) and (d). Fig. 3 (b) shows the BLAST calculation of $L_C(t)$ and $H(t)$ for the MoWiTT and the passive cell. In both cases, during the daytime $H(t)$ is approximately 40% of the total solar gain, which is the origin of the value of 0.4 taken for α in the simplified discussion above. Both curves for the MoWiTT and the $L_C(t)$ curve for the passive cell were multiplied by the 5% assumed accuracy to produce the time-dependent absolute errors, $\delta L_C(t)$ and $\delta H(t)$. For the passive cell, during the daylight hours the values of $H(t)$ were corrected for the effects of the moving patch of sunlight as described above. These are shown as points in Fig. 3 (c), with the derived errors $\delta H(t)$ shown as error bars on the points. As can be seen, the points show sizable deviations from the BLAST-calculated curve (assumed to be the true value) which are considerably larger than the range expected for random errors. This is due to the incorrect weighting of essentially point measurements of the wall heat flux as the patch of direct sunlight moves around the wall. Only the size of the deviations is significant; a different sun angle or arrangement of the sensor grid would produce a different pattern

of deviations from the curve--possibly even in the opposite direction. This is a graphic demonstration of the type of systematic error that may arise in daytime measurements attempted with an inadequate measurement system.

In Fig. 3(d), the values $L_C(t)$ and $H(t)$ are combined using Eq. (1) to produce the window net energy flow, $W(t)$. The errors $\delta L_C(t)$ and $\delta H(t)$ are added in quadrature to produce the measurement error $\delta W(t)$. For the MoWiTT these results are shown as a curve surrounded by an error band (which is too small to be visible during nighttime hours); for the passive cell they are represented as points with error bars.

This calculation reveals no surprises for the MoWiTT, which maintains approximately 5% accuracy throughout the day. This is because, for this sample and design day, one effect--solar gain during the day, transmissive loss at night--clearly dominates. For the case of a north-facing window one might see degraded accuracy during the daytime. For the passive cell, however, two effects may be observed which point up the advantage of the MoWiTT: First, during the night measurements the accuracy of the measurement is degraded to the approximate range $35\% \leq (\delta W/W) \leq 50\%$. This is because the nighttime measurement of $W(t)$ involves taking the difference between measurements of two large numbers, as can be seen from Fig. 3(b). Second, large systematic errors of up to 30% occur during the daytime measurement. Since these are much larger than the random error expected, measurements with this facility would result in erroneous conclusions about both the magnitude and the shape of the curve $W(t)$.

Conclusions

We conclude that direct measurement of the net energy flow through fenestrations of moderate complexity under realistic conditions is a difficult undertaking requiring a specialized measurement facility. One such facility, the MoWiTT, is designed to be capable of accurate measurements on fenestrations with thermal resistance up to 10 times that of single glazing and shading coefficient down to 0.1. This represents a significant advance in the state of the art in fenestration measurement.

The first module of the MoWiTT, undergoing calibration at LBL, is shown in Fig. 4.

Acknowledgement

This work was supported by the Assistant Secretary for Conservation and Renewable Energy, Office of Energy Research and Development, Building Systems Division of the U.S. Department of Energy under Contract No. DE-AC03-76SF00098.

References

1. DOE-2 Engineers Manual, Building Energy Analysis and Group Q-11, Los Alamos National Laboratory, Report No. EEB-DOE-2 81-2, LBL-11353, LA-8520-M, November, 1982.
2. D.C. Hittle, "The Building Load Analysis and System Thermodynamics (BLAST) Program Version 1.0: Users Manual, Vol. 1," Report no. CERL-TR-E-153, U.S. Army Construction Engineering Research Laboratory, Champaign, Ill., June 1979. BLAST is trademarked by the Construction

Engineering Research Laboratory, U.S. Department of the Army, Champaign, Illinois.

3. Jeffrey F. Lowinski, "Thermal Performance of Wood Windows and Doors," ASHRAE Transactions, Vol. 85, pt. 1, 1979.
4. Stephen J. Rennekamp, "U-Value Testing of Windows Using a Modified Guarded Hot Box Technique," ASHRAE Transactions, Vol. 85, pt. 1, p. 1979.
5. M.E. McCabe and E. Hancock, "Initial Results from Testing Passive Solar Components in the NBS Calorimeter," Proceedings of the Passive and Hybrid Solar Energy Update, U.S. Department of Energy, Report No. CONF-830980, Washington, D.C., November, 1983.
6. John I. Yellott, "Shading Coefficients and Sun-Control Capability of Single Glazing," ASHRAE Transactions, Vol. 72, pt. 1, p.72, 1966.
7. George V. Parmchee, Warren W. Aubele, and Richard G. Huelscher, "Measurements of Solar Heat Transmission Through Flat Glass," Heating, Piping and Air Conditioning, p.158, January, 1948.
8. William B. May, Jr. and Lawrence G. Spielvogel, "Analysis of Computer-Simulated Thermal Performance of the Norris Cotton Federal Office Building," ASHRAE Transactions, Vol. 87, pt. 2, p.1207, 1981.
9. Tamami Kusuda, E. Thomas Pierce, and J.W. Bean, "Comparison of Calculated Hourly Cooling Load and Attic Temperature with Measured Data for a Houston Test House," ASHRAE Transactions, Vol. 87, pt. 2, p.1185, 1981.

10. R. Judkoff, D. Wortman and J. Burch, "Measured Versus Predicted Performance of the SERI Test House: A Validation Study," Proceedings of the Passive and Hybrid Solar Energy Update, U.S. Department of Energy, Report no. CONF-830980, Washington, D.C., November, 1983.
11. F. Bauman, B. Andersson, W.L. Carroll, R. Kammerud, and W.E. Friedman, "Verification of BLAST by Comparison with Measurements of a Solar-Dominated Test Cell and a Thermally Massive Building," Journal of Solar Energy Engineering, Vol. 105, p. 207, 1983.
12. T. E. Richtmeyer, W.B. May, C.M. Hunt, and J.E. Hill, "Thermal Performance of the Norris Cotton Federal Building in Manchester, New Hampshire," Thermal Performance of the Exterior Envelopes of Buildings, ASHRAE SP 28, American Society of Heating, Refrigerating and Air Conditioning Engineers, Inc., New York NY, pp. 781-800, 1981.
13. J. H. Klems and D. DiBartolomeo, "Large-area, High-Sensitivity Heat-Flow Sensor," Rev. Sci. Instrum. 53, (10), p. 1609, 1982.
14. J. H. Klems, "Use of Large-Area Heat-Flow Meters to Measure Building Heat Flows," Thermal Performance of the Exterior Envelopes of Buildings, II, ASHRAE SP 38, American Society of Heating, Refrigerating and Air Conditioning Engineers, Inc., Atlanta GA, p. 734, 1983.
15. J. H. Klems and D. DiBartolomeo, "Full-sized, Quantity-Produced Large-Area Heat Flow Sensors," to be published.

Appendix A: Glossary of Symbols

Term	Definition
------	------------

B	Shading coefficient of the fenestration.
---	--

C	Volume-weighted average of ρC_p for all thermal mass contained in E.
---	--

C_p	Specific heat at constant pressure.
-------	-------------------------------------

E	Denotes an imaginary surface lying just below the physical inner surface of the exterior envelope of V; also, the area of that surface.
---	---

f	Fluid flow rate (volumetric).
---	-------------------------------

F	Area of fenestration.
---	-----------------------

F'	Fenestration area illuminated by sunlight
------	---

G	Gross floor area of the building in question.
---	---

H	Envelope heat flow across surface E.
---	--------------------------------------

H_c	Heat flow by conduction/convection between the exterior envelope and the air inside E.
-------	--

I	Heat transfer by infiltration into V.
---	---------------------------------------

J_o	A reference solar intensity (W/m^2) incident on the structure and transmitted through single glazing.
-------	---

L_c	Rate of removal of energy from building space by climate-control system (space load). Negative L_c is heating load.
-------	---

Term	Definition
Q_c	Conductive/convective part of Q_w .
Q_r	Radiative part of Q_w .
Q_w	Heat leaving the innermost surface of the fenestration by conduction, convection, and (long-wave) radiation.
R	Dimensionless thermal resistance of fenestration, defined as the ratio of thermal resistance to that of single glazing.
R_e	Dimensionless thermal resistance of envelope, defined as the ratio of the envelope thermal resistance to that of single glazing.
S_w	Energy leaving the innermost surface of the fenestration as radiation in the visible and solar infrared bands.
T	Temperature.
T_A	Weighted mean temperature of all material inside E.
T_i	Inlet fluid temperature.
T_e	Exit fluid temperature.
t	Time.
U	Thermal transmittance.
U_o	Thermal transmittance of single glazing.
V	Volume enclosed by surface E.
W	Energy flow rate through the fenestration.

Term	Definition
z_i	Internal load per unit floor area.
α	Fraction of solar energy incident on interior building envelope surface that flows across E.
δ	Operator denoting "measurement uncertainty in"; e.g., δW denotes measurement uncertainty in W.
ΔT	Difference between interior and exterior air temperatures.
ΔT_G	Difference between interior and guard air temperatures.
ΔT_S	Difference between interior air temperature and exterior sol-air temperature.
\leftarrow	Symbol used to denote an infinitesimal difference.
ρ	Density.
ζ	Parameter accounting for thermal lags between fenestration/envelope heat flows and space load.
ξ	Fraction of exterior envelope illuminated by sunlight.
τ	Data sampling time period.

Appendix B. Derivation of Measurement Accuracy Requirements From the Tables

We discuss here the details of deriving accuracy requirements from the tables. As an example, we consider the derivation of our statements about the seven-story office building in the heating mode. Substitution into Table 1 of the values given in the text for V/F , C , δT_A , U_o , τ , ΔT , E/F , a, ζ , G/F and z_I yields the entries in the nighttime column of Table 2. For single glazing $R = 1$, and addition of the column entries in quadrature yields $\delta W/W$:

$$\begin{aligned} \left(\frac{\delta W}{W}\right)^2 &= (0.14)^2 (\delta T_A)^2 + (0.15)^2 \left(\frac{\delta H}{H}\right)^2 \\ &+ (1.5)^2 \left(\frac{\delta a}{a}\right)^2 + (-1.8)^2 \left(\frac{\delta L_c}{L_c}\right)^2 \end{aligned}$$

If we require that the overall accuracy be $\delta W/W \leq 10\%$ and allow an equal contribution to the uncertainty from each of the four independent sources of error, then, for example:

$$(2.0) \left(\frac{\delta L_c}{L_c}\right) \leq \frac{0.1}{2},$$

yielding $(\delta L_c/L_c) \leq 3\%$. The same requirement applied to each of the other terms in the sum yields $(\delta a/a) \leq 3\%$, $(\delta H/H) \leq 33\%$ and $\delta T_A \leq 0.4^\circ\text{C}$, as given in the text. Of course, if the measured accuracy on one of the variables (H , L_c , etc.) is much better than the requirement, then that term may be dropped from the sum and the uncertainty shared equally between the remaining terms. The limit of this process is obviously the case where a single error dominates all the others.

Table 1. Error Sources in Fenestration Heat Flow Measurement

(a) Nighttime	
Source	Contribution to $\delta W/W$
Space Heat Content	$R(\frac{V}{F}) \frac{\sqrt{2} C \delta T_A}{U_0 \tau \Delta T}$
Envelope Conduction	$\frac{R}{R_E} (\frac{E}{F}) (\frac{\delta H}{H})$
Infiltration	$R(\frac{V}{F}) \frac{Ca}{U_0} (\frac{\delta a}{a})$
Space Load	$\left\{ \xi \left[1 + \frac{H}{W} \right] + \frac{I}{W} - R(\frac{G}{F}) \frac{z_I}{U_0 \Delta T} \right\} (\frac{\delta L_C}{L_C})$
(b) Daytime	
Source	Contribution to $\delta W/W$
Space Heat Content	$(\frac{1}{B}) (\frac{V}{F}) \frac{\sqrt{2} C V \delta T_A}{J_0 \tau}$
Envelope Conduction	$\alpha (\frac{\delta H}{H})$
Infiltration	$(\frac{1}{B}) (\frac{V}{F}) \frac{Ca \Delta T}{J_0} (\frac{\delta a}{a})$
Space Load	$\left\{ (1-\alpha) + \frac{I}{W} + (\frac{1}{B}) \xi (\frac{E}{F}) \frac{\Delta T_S U_0}{R_E J_0} + (\frac{1}{B}) (\frac{G}{F}) \frac{z_I}{J_0} \right\} (\frac{\delta L_C}{L_C})$

Table 2. Error Source Contributions to $\delta W/W$ in Two Sample Buildings

(a) Single-Story Residence		
Source	Nighttime	Daytime
Heat Content	$0.051 R \delta T_A$	$0.014 \left(\frac{1}{B}\right) \delta T_A$
Envelope	$0.92 R \left(\frac{\delta H}{H}\right)$	$0.4 \left(\frac{\delta H}{H}\right)$
Infiltration	$0.54 R \left(\frac{\delta a}{a}\right)$	$0.15 \left(\frac{1}{B}\right) \left(\frac{\delta a}{a}\right)$
Climate-control System	$(1 + 1.5 R) \left(\frac{\delta L_C}{L_C}\right)$	$[0.6 - 0.12 \left(\frac{1}{B}\right)] \left(\frac{\delta L_C}{L_C}\right)$
(b) Seven-Story Office Building		
Source	Nighttime	Daytime
Heat Content	$0.14 R \delta T_A$	$0.078 \left(\frac{1}{B}\right) \delta T_A$
Envelope	$0.29 R \left(\frac{\delta H}{H}\right)$	$0.4 \left(\frac{\delta H}{H}\right)$
Infiltration	$1.5 R \left(\frac{\delta a}{a}\right)$	$0.83 \left(\frac{1}{B}\right) \left(\frac{\delta a}{a}\right)$
Climate-control System	$[0.5 - 2.5 R] \left(\frac{\delta L_C}{L_C}\right)$	$[0.6 + 1.5 \left(\frac{1}{B}\right)] \left(\frac{\delta L_C}{L_C}\right)$

Table 3. Estimated Error Source Contributions to $\delta W/W$ for an R-40 Test Cell

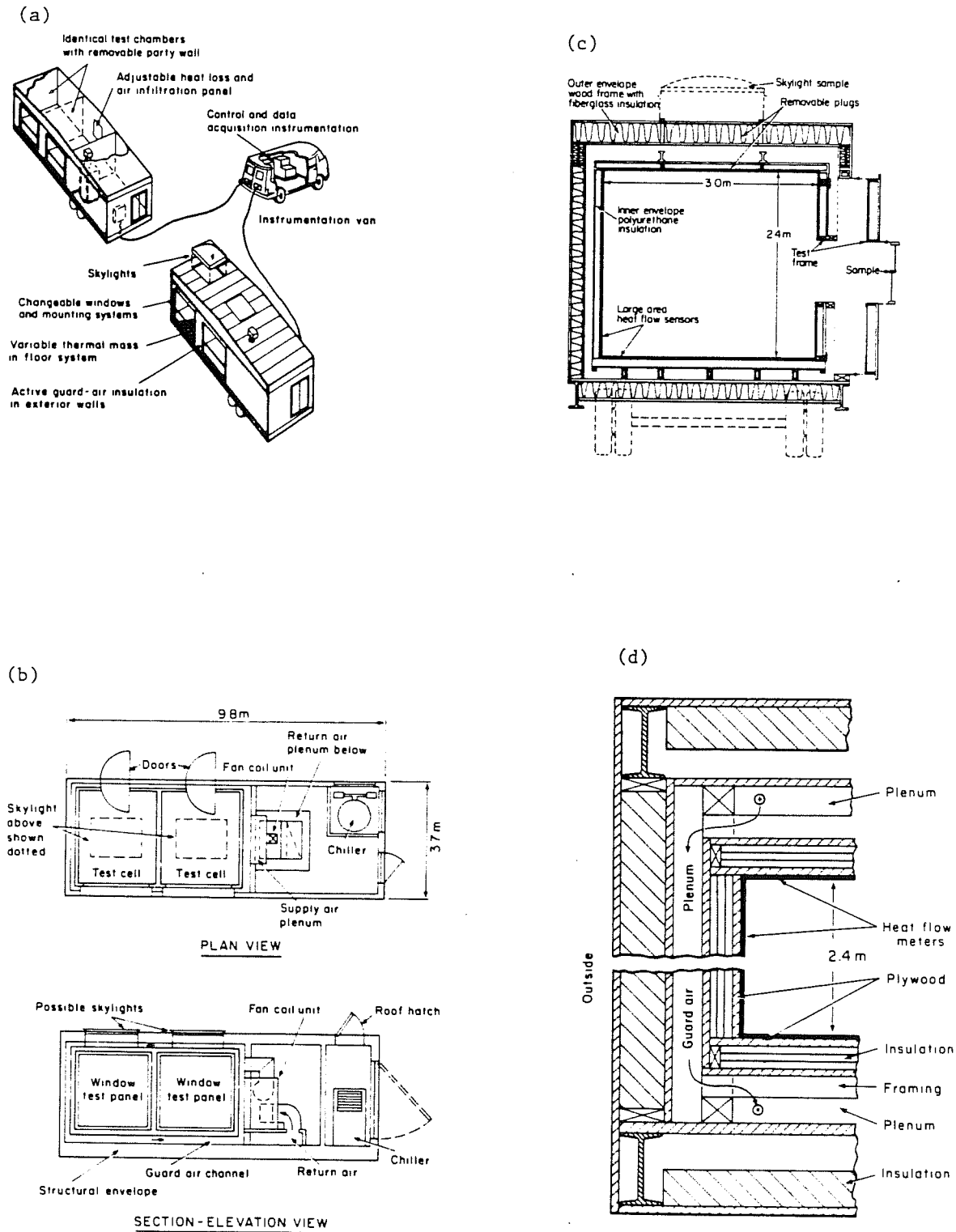
(a) Small Window

Source	Nighttime	Daytime
Air Heat Content	$0.08R \delta T_A$	$0.01(\frac{1}{B}) \delta T_A$
Envelope Conduction	$1.0R(\frac{\delta H}{H})$	$0.4(\frac{\delta H}{H})$
Climate Control System	$(1 + R)(\frac{\delta L_C}{L_C})$	$[0.6 + 0.02(\frac{1}{B})](\frac{\delta L_C}{L_C})$

(b) Large Window

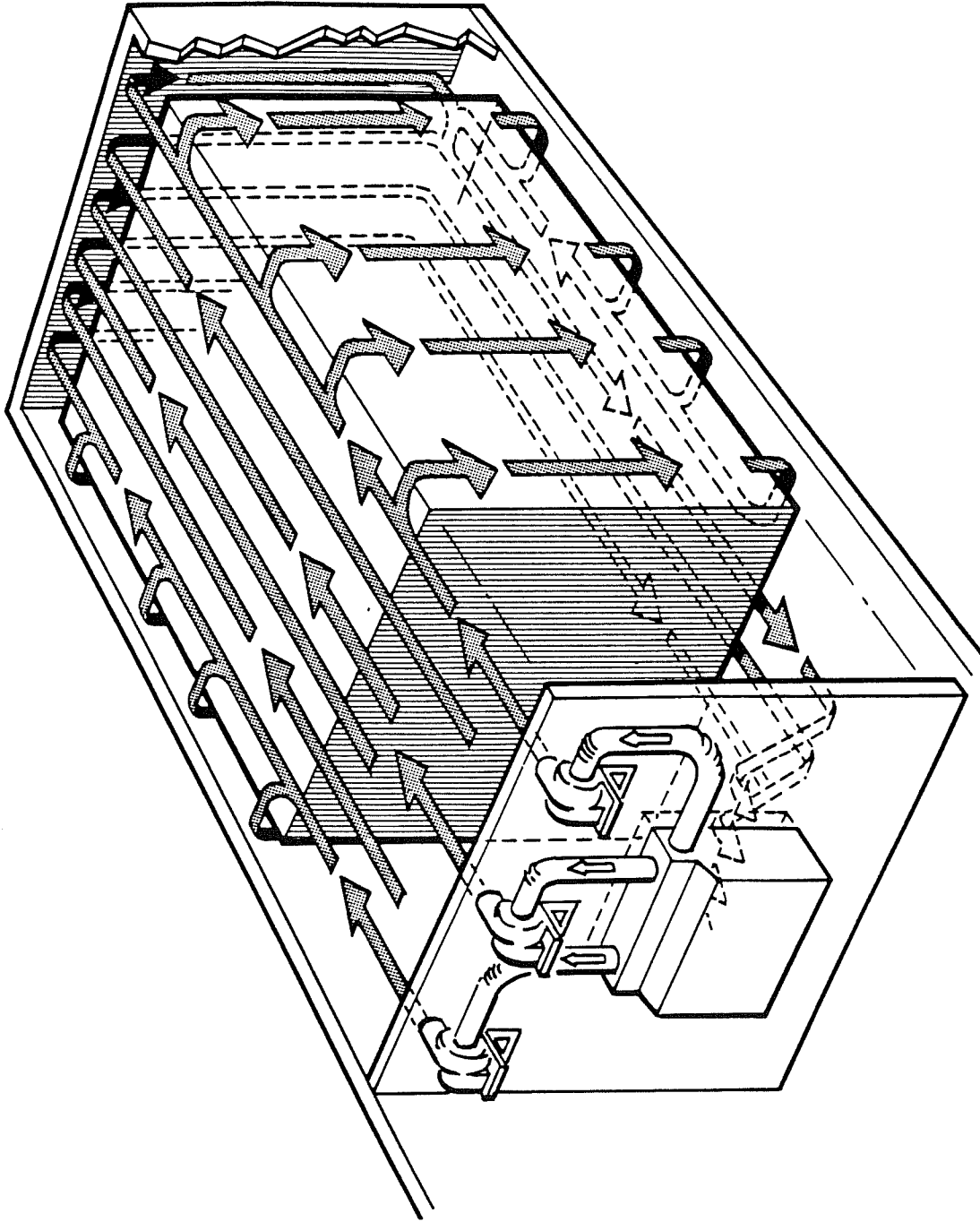
Source	Nighttime	Daytime
Air Heat Content	$0.01R \delta T_A$	$0.002(\frac{1}{B}) \delta T_A$
Envelope Conduction	$0.15R(\frac{\delta H}{H})$	$0.4(\frac{\delta H}{H})$
Climate Control System	$(1 + 0.15R)(\frac{\delta L_C}{L_C})$	$[0.6 + 0.003(\frac{1}{B})](\frac{\delta L_C}{L_C})$

Table 4. Estimated Fractional Error Magnitudes in MoWITT		
(a) Expressions		
(1) Nighttime		
Source	Contribution to $\delta W/W$	
Air Heat Content	$\frac{\sqrt{2}C}{\tau U_o \Delta T} (\frac{V}{F}) R \delta T_A$	
Envelope Heat Flow	$(\frac{E}{F}) (\frac{R}{R_E}) (\frac{\Delta T_G}{\Delta T}) (\frac{\delta H}{H})$	
Infiltration	$\frac{C}{U_o} (\frac{V}{F}) (\frac{\Delta T_G}{\Delta T}) R \delta a$	
Climate-Control System	$\zeta [1+(\frac{E}{F}) (\frac{R}{R_E}) (\frac{\Delta T_G}{\Delta T})] (\frac{\delta L_C}{L_C})$	
(2) Daytime		
Source	Contribution to $\delta W/W$	
Air Heat Content	$\frac{\sqrt{2}C}{J_o} \tau (\frac{V}{F}) \frac{1}{B} \alpha T_A$	
Envelope Heat Flow	$\alpha (\frac{\delta H}{H})$	
Infiltration	$C \frac{\Delta T_G}{J_o} (\frac{V}{F}) (\frac{1}{B}) \delta a$	
Climate-Control System	$(1-\alpha) \frac{\delta L_C}{L_C}$	
(b) Numerical Calculations		
Source	Contribution to $\delta W/W$	
	Nighttime	Daytime
Air Heat Content	$0.10 R \delta T_A$	$0.014 \frac{1}{B} \delta T_A$
Envelope Heat Flow	$0.11 R \frac{\delta H}{H}$	$0.4 \frac{\delta H}{H}$
Infiltration	$0.10 R \delta a$	$0.015 \frac{1}{B} \delta T_a$
Climate-Control System	$(1 + 0.11 R) (\frac{\delta L_C}{L_C})$	$0.6 (\frac{\delta L_C}{L_C})$



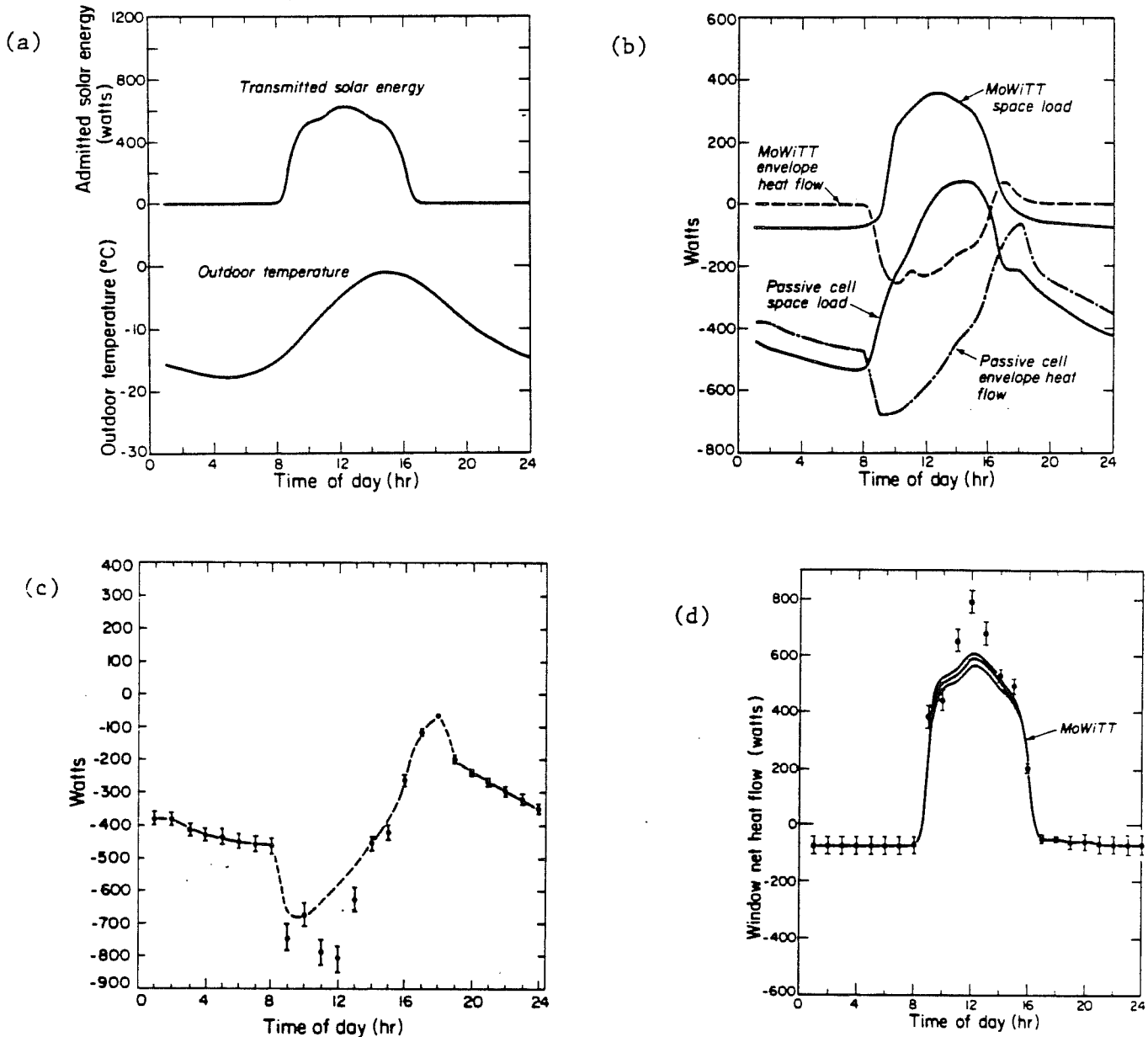
XBL 811-125A

Figure 1. Design of the Mobile Window Thermal Test (MoWiTT) facility. (a) Planned field configuration. (b) Layout of a test module. (c) Cross-section through the center of a test chamber, showing mounting of alternative window or skylight systems. (d) Detailed envelope cross-section.



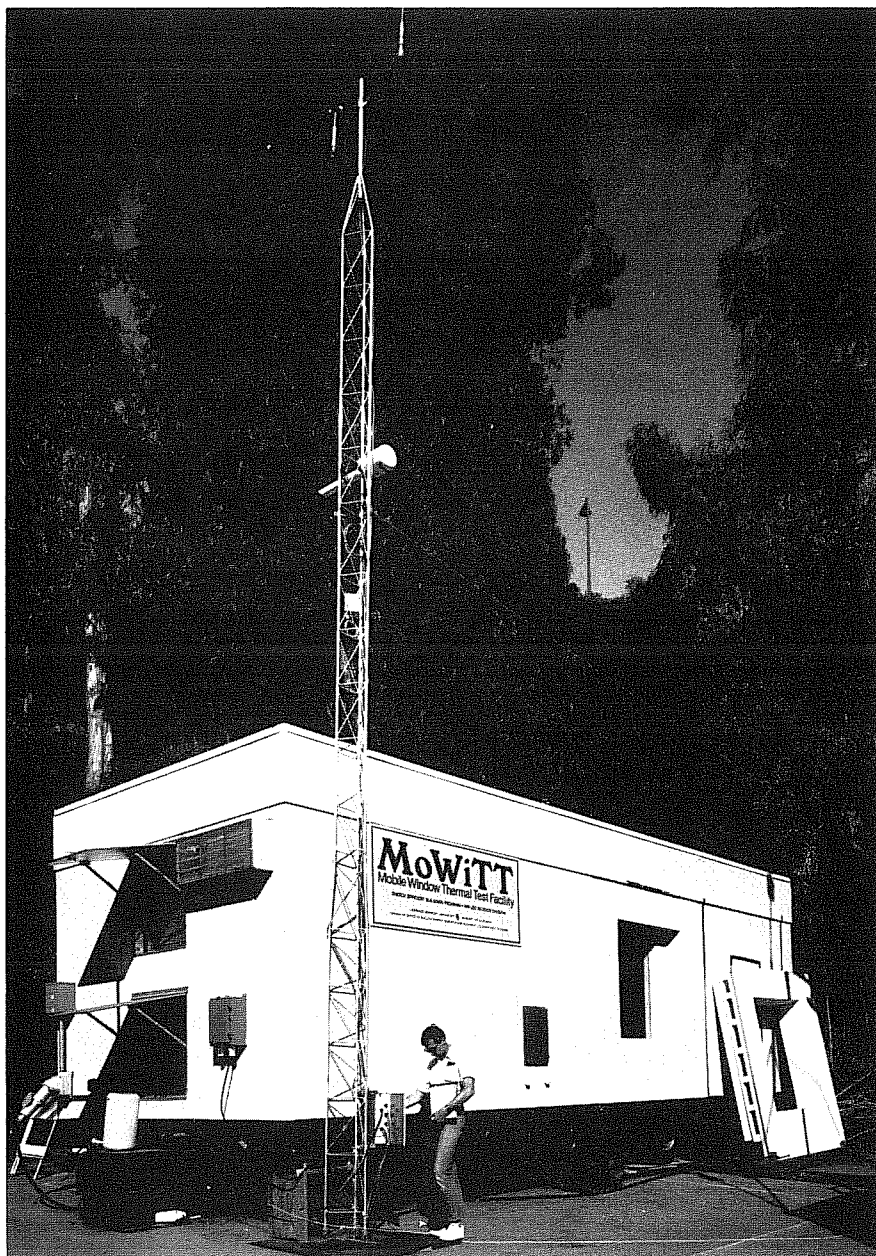
XBL 842-9412

Figure 2. MoWITT Guard System, showing circulation of forced-flow, temperature-controlled air around the two test rooms.



XBL 8110-1404A

Figure 3. BLAST Simulation of a triple-glazed window measurement comparing the MoWiTT and a passive test cell. (a) Assumed outdoor temperature and solar energy transmitted through the window. Indoor temperature is assumed to be a constant 20°C. (b) Calculated space loads, $L_c(t)$, (solid curves) and envelope heat flows, $H(t)$, (dashed curves) for the MoWiTT and for the passive cell. (c) Measurement of envelope heat flow in the passive cell. Dashed curve: BLAST calculation of the envelope heat flow; points with error bars: envelope heat flow, which would be measured with the heat-flow meter grid described in the text. (d) Derived values for the net heat flow, W , through the window. Solid curves are the mean, +1 standard deviation, and -1 standard deviation, for measurements by the MoWiTT. Points with error bars are the corresponding quantities for the passive cell with heat-flow meter grid.



CBB 830-9555

Figure 4. The first MoWiTT measurement module during calibration at Lawrence Berkeley Laboratory.

